arXiv:cond-mat/0411251v1 [cond-mat.mtrl-sci] 10 Nov 2004

Optical properties of random alloys : Application to $Cu_{50}Au_{50}$ and $Ni_{50}Pt_{50}$

Kamal Krishna Saha* and Abhijit Mookerjee†
S. N. Bose National Centre for Basic Sciences. Block-JD, Sector-III, Salt Lake City, Kolkata-700098, India.

(Dated: February 2, 2008)

In an earlier paper [K. K. Saha and A. Mookerjee, Phys. Rev. B **70** (2004) (in press) or, cond-mat/0403456] we had presented a formulation for the calculation of the configuration-averaged optical conductivity in random alloys. Our formulation is based on the augmented-space theorem introduced by one of us [A. Mookerjee, J. Phys. C: Solid State Phys. **6**, 1340 (1973)]. In this communication we shall combine our formulation with the tight-binding linear muffin-tin orbitals (TB-LMTO) technique to study the optical conductivities of two alloys $Cu_{50}Au_{50}$ and $Ni_{50}Pt_{50}$.

PACS numbers: 71.23.-k

I. INTRODUCTION

In this communication we propose to study the optical properties of disordered CuAu and NiPt 50-50 alloys from a first principle approach. We have chosen these two alloy systems because of several reasons : for CuAu, the bunch of d-like states sits about 1 eV below the Fermi level. For low photon energies, therefore, optical conductivity is dominated by the intra-band transitions within $s-p$-like states, which are extended and rather free electron-like. As a consequence, the optical conductivity for low photon energies below $\simeq 1$ eV should have a Drude like behaviour. For higher photon energies inter-band transitions between the occupied d-states and the higher unoccupied states begin to take over. In sharp contrast, the Fermi energy of NiPt almost straddles the d-like peak. For this alloy the Drude behaviour should be confined to a very narrow low photon energy range. This contrasting behaviour should be reflected in our results. Moreover, in both the two alloy systems there is a large size mismatch between the constituents. This indicates that the standard single site mean-field theories would be inadequate to capture the effect of this large size-mismatch. These alloy systems are therefore ideal to illustrate the advantages of the augmented-space recursion (ASR) method proposed by us[1].

Earlier theoretical work on optical conductivity for random alloys began with Velický[2] based on the single site coherent potential approximation (CPA) in an empirical tight-binding model alloy. Butler[3] extended the ideas and combined the CPA with the first-principles Korringa-Kohn-Rostocker (KKR) technique. Banhart[4] used the KKR-CPA to study the optical conductivity of AgAu alloys. This alloy system has close resemblance to CuAu. Banhart found discrepancies of his theoretical results with experiment[5,6] and argued that various factors could be responsible : use of the density functional and the single-site mean-field approximations in theory and effects of surfaces, their roughness, possible adsorbates and presence of large stresses in the samples, in the experiments. There have been a few more theoretical studies of optical properties of random alloys : Rhee *et al.*[7] on CoAl, Uba *et al.*[8] on CoPt and Rhee *et al.*[9] on Ni_3Al. These works all base their approach on a large super-cell method to take care of the disorder. The method is brute force and less satisfactory than the CPA or ASR.

In an earlier paper[10] we had presented a formulation for obtaining the configuration averaged optical conductivity for random binary alloys. We had chosen as our basis the minimal set of the tight-binding linear muffin-tin orbitals method[11,12]. Configuration averaging over various random atomic arrangements had been carried out using the augmented-space formalism (ASF) introduced by us earlier for the study of electronic properties of disordered systems[13,14]. The ASF goes beyond the usual single site mean-field approaches and takes into account configuration fluctuations about the mean-field. We shall present here a summary of the results derived in the earlier paper[10]. In linear response theory, at zero temperature, the real part of the optical conductivity of a disordered alloy is given by the Kubo-Greenwood expression :

$$\sigma(\omega) \;=\; \frac{S(\omega)}{\omega} \tag{1}$$

where, the configuration averaged current-current correlation function $\ll S(\omega) \gg$ is given by :

$$\frac{1}{3\pi}\sum_{\gamma} \mathrm{Tr} \int dE \left\langle \mathbf{j}_\gamma \mathrm{Im}\{\mathbf{G}^v(E)\}\mathbf{j}_\gamma^\dagger \; \mathrm{Im}\{\mathbf{G}^c(E+\omega)\}\right\rangle \tag{2}$$

If we define

$$\ll S_\gamma(z_1,z_2) \gg = \mathrm{Tr}\; \left\langle \; \mathbf{j}_\gamma \; \mathbf{G}^v(z_1) \; \mathbf{j}_\gamma^\dagger \; \mathbf{G}^c(z_2)\right\rangle \tag{3}$$

then, using the Herglotz properties of the Green function, the correlation function becomes

$$\begin{aligned} \ll S(\omega) \gg = \frac{1}{12\pi}\sum_\gamma \int dE \;\; \big[\; & \mathcal{S}_\gamma(E^-,E^+ +\omega) \\ & + \mathcal{S}_\gamma(E^+,E^- +\omega) - \mathcal{S}_\gamma(E^+,E^+ +\omega) \\ & -\mathcal{S}_\gamma(E^-,E^- +\omega)\big] \end{aligned} \tag{4}$$

where

$$f(E^\pm) \;=\; \lim_{\delta\to 0} f(E \pm i\delta).$$

The formulation we presented in our earlier paper[10] was based on the disordered induced scattering leading to the renormalization of the propagator $\mathbf{G}$ as well as the current terms $\mathbf{j}$. The dominant contributions to the configuration averaged correlation function was due to joint fluctuations of an averaged current and two electron propagators :

$$\ll S_\gamma^{(0)}(z_1,z_2) \gg = \int_{\rm BZ} \frac{d^3\mathbf{k}}{8\pi^3} \ \ll \mathbf{j}_\gamma(\mathbf{k}) \gg \ll \mathbf{G}^v(\mathbf{k},z_1) \gg \ll \mathbf{j}_\gamma(\mathbf{k}) \gg^\dagger \ll \mathbf{G}^c(\mathbf{k},z_2) \gg . \tag{5}$$

We have also shown that disorder scattering renormalizes that averaged current to an effective current term and the average propagator to a configuration averaged propagator beyond the CPA approximation. We expressed the effective current in terms of the self-energy as :

$$\begin{aligned}\mathbf{J}_\gamma^{\rm eff}(\mathbf{k},z_1,z_2) \ &= \ll \mathbf{j}_\gamma(\mathbf{k}) \gg + 2\left[\mathbf{\Sigma}(\mathbf{k},z_2)\ \mathbf{f}(z_2)\ {\mathbf{j}_\gamma^{(1)}}^\dagger(\mathbf{k}) \ + \ {\mathbf{j}_\gamma^{(1)}}^\dagger(\mathbf{k})\ \mathbf{f}(z_1)\ \Sigma(\mathbf{k},z_1)\right] \\ &+ \Sigma(\mathbf{k},z_2)\ \mathbf{f}(z_2)\ \mathbf{j}_\gamma^{(2)}(\mathbf{k})\ \mathbf{f}(z_1)\ \Sigma(\mathbf{k},z_1).\end{aligned} \tag{6}$$

and the contribution to the effective current to the correlation function was :

$$\ll S_\gamma^{(1)}(z_1,z_2) \gg \ = \ \int_{\rm BZ} \frac{d^3\mathbf{k}}{8\pi^3} \ {\rm Tr}\left[\mathbf{J}_\gamma^{\rm eff}(\mathbf{k},z_1,z_2) \ll \mathbf{G}^v(\mathbf{k},z_1) \gg \mathbf{J}_\gamma^{\rm eff}(\mathbf{k},z_1,z_2)^\dagger \ll \mathbf{G}^c(\mathbf{k},z_2) \gg\right]. \tag{7}$$

The contribution of joint fluctuations between the two current terms and one propagator was given by

$$\begin{aligned}\ll S_\gamma^{(2)}(z_1,z_2) \gg \ &= \ 4 \int_{\rm BZ} \frac{d^3\mathbf{k}}{8\pi^3} \ {\rm Tr}\Big[\ \mathbf{j}_\gamma^{(1)}(\mathbf{k})\ \mathbf{f}(z_1)\ \Sigma(\mathbf{k},z_1)\ \mathbf{f}(z_1)\ {\mathbf{j}_\gamma^{(1)}}^\dagger(\mathbf{k}) \ \ll \mathbf{G}(\mathbf{k},z_2) \gg \\ &+ {\mathbf{j}_\gamma^{(1)}}^\dagger(\mathbf{k})\ \mathbf{f}(z_2)\ \Sigma(\mathbf{k},z_2)\ \mathbf{f}(z_2)\ \mathbf{j}_\gamma^{(1)}(\mathbf{k}) \ \ll \mathbf{G}(\mathbf{k},z_1) \gg \Big].\end{aligned} \tag{8}$$

The vertex correction terms in the ladder approximation contributed :

$$\ll S_\gamma^{\rm ladder}(z_1,z_2) \gg = \ {\rm Tr} \sum_{L_1L_2} \sum_{L_3L_4} \Gamma_\gamma^{L_1L_2}(z_1,z_2)\ \Lambda_{L_2L_4}^{L_1L_3}\ \widehat{\Gamma}_\gamma^{L_3L_4}(z_1,z_2) = \ {\rm Tr}\ \mathbf{\Gamma}_\gamma(z_1,z_2) \otimes \widehat{\mathbf{\Gamma}}_\gamma(z_1,z_2)\ \Lambda(z_1,z_2). \tag{9}$$

where

$$\int_{\rm BZ} \frac{d^3\mathbf{k}}{8\pi^3}\ \mathbf{G}(\mathbf{k},z_2)\ \mathbf{J}_\gamma^{\rm eff}(\mathbf{k},z_1,z_2)\ \mathbf{G}(\mathbf{k},z_1) = \mathbf{\Gamma}_\gamma(z_1,z_2)$$

$$\int_{\rm BZ} \frac{d^3\mathbf{k'}}{8\pi^3}\ \mathbf{G}(\mathbf{k'},z_1)\ \mathbf{J}_\gamma^{\rm eff}(\mathbf{k'},z_1,z_2)^\dagger \mathbf{G}(\mathbf{k'},z_2) = \widehat{\mathbf{\Gamma}}_\gamma(z_1,z_2).$$

and

$$\lambda_{L_3L_4}^{L_1L_2}(z_1,z_2) = \int_{\rm BZ} \frac{d^3\mathbf{k}}{8\pi^3}\ G_{L_3L_4}(\mathbf{k},z_1)\ G_{L_2L_1}(\mathbf{k},z_2)$$

$$\omega_{L_3L_4}^{L_1L_2} = W_{L_3}^{L_1}\ \delta_{L_1L_2}\ \delta_{L_3L_4}$$

$$W_{L'}^{L} = F_L(z_2)\left[\delta_{LL'} + 2\sum_{L''}\Big[B_{L''}(z_1)\ G_{RL'',RL'}(z_1) + B_{L''}(z_2)\ G_{RL'',RL'}(z_2)\Big]\right] F_{L'}(z_1).$$

$$F_L(z) = \sqrt{xy}\ d\left(\frac{C_L - z)}{\Delta_L}\right) / \ll 1/\Delta_L \gg$$

$$B_L(z) = (y-x)\ d\left(\frac{C_L - z)}{\Delta_L}\right) / \ll 1/\Delta_L \gg$$

Here x, y are the concentrations of the component atoms, C,Δ are the standard potential parameters of the TB-LMTO and $d(f) = f_A - f_B$. These super-matrices in

Alloy	Lowest energy lattice const (Å)	Vegard's Law lattice const (Å)
$Cu_{50}Au_{50}$	7.31	7.26
$Ni_{50}Pt_{50}$	7.09	7.03

TABLE I: Lowest energy and Vegard's Law lattice constants for CuAu and NiPt.

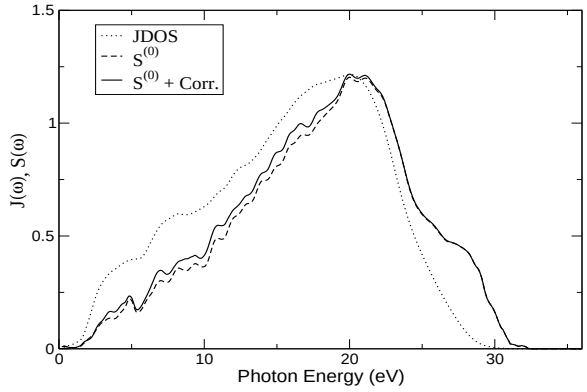


FIG. 1: The configuration averaged joint density of states and correlation function for CuAu (50-50) alloy shown as a function of the photon energy.

$\{L\}$ space are written as $\underline{\underline{\lambda}}$ and $\underline{\underline{\omega}}$. The full ladder vertex may now be written as

$$\begin{aligned}\underline{\underline{\Lambda}}(z_1,z_2) &= \underline{\underline{\omega}} + \underline{\underline{\omega}}\,\underline{\underline{\lambda}}\,\underline{\underline{\omega}} + \underline{\underline{\omega}}\,\underline{\underline{\lambda}}\,\underline{\underline{\omega}}\,\underline{\underline{\lambda}}\,\underline{\underline{\omega}} + \dots \\ &= \underline{\underline{\omega}}\left(\underline{\underline{I}} - \underline{\underline{\lambda}}(z_1,z_2)\,\underline{\underline{\omega}}\right)^{-1} \qquad (10)\end{aligned}$$

Including all sorts of corrections the averaged correlation function is then :

$$\ll S_\gamma(z_1,z_2) \gg = \ll S_\gamma^{(1)}(z_1,z_2) \gg + \ll S_\gamma^{(2)}(z_1,z_2) \gg + \ll S_\gamma^{\rm ladder}(z_1,z_2) \gg$$

II. RESULTS AND DISCUSSION

We have begun our study with the self-consistent TB-LMTO-ASR calculation on NiPt and CuAu 50-50 alloys. We have minimized the energy with respect to the variation in the average lattice constant for both the alloys. The table shows the lowest energy lattice constants and compares them with the averaged or Vegard's law results. As expected, because of the large size difference between the constituents there is a "bowing" effect which is most prominent at the 50-50 alloys. The lowest energy lattice constant for both the alloys is greater than the Vegard's law predictions.

Figure 1 shows the comparison between the scaled joint density of states (JDOS) and the averaged correlation function for a CuAu (50-50) alloy. From the figure it is clear that the transition rate is dependent both on the initial and the final energies, throughout the frequency range of interest. That is :

$$S(\omega) \neq |T|^2\ J(\omega)$$

where

$$J(\omega) = \int dE \int \frac{d^3\mathbf{k}}{8\pi^3}\ {\rm Tr}\langle \mathbf{G}^c(\mathbf{k},E)\mathbf{G}^v(\mathbf{k},E+\omega)\rangle.$$

The Fig. 1 also shows that the disorder corrections to the current and the vertex correction are rather small and become negligible beyond photon energies of about 22 eV.

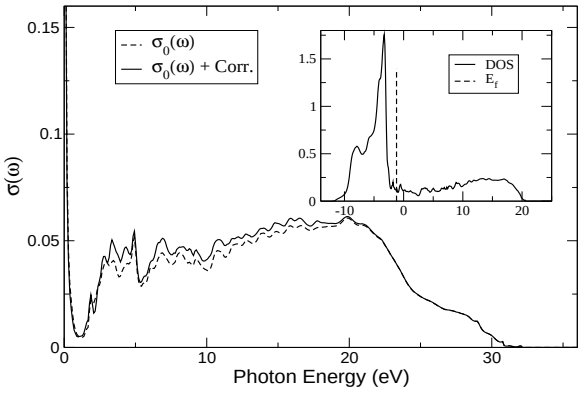


FIG. 2: Averaged optical conductivity, $\sigma_0(\omega) = S^{(0)}/\omega$, and the density of states for a CuAu (50-50) alloy. The corrections to the optical conductivity are shown in Eqs. (6-9).

Figure 2 shows the optical conductivity $\sigma(\omega)$ for CuAu (50-50) alloy. The inset shows the configuration averaged density of states for the same alloy. The edge of the d-band complex is clearly seen to lie about 1 eV below the Fermi energy. The optical conductivity rapidly decreases as we increase the photon energy from zero upwards. This decrease continues until about 1 eV and then the conductivity rises again and has considerable structure as also shown in the correlation function for these photon energies (Fig. 1).

Figure 3 shows the optical conductivity with a Drude fit $[\sigma^D(\omega) = \sigma(0)/(1+(\omega\tau)^2),\ \text{with}\ \sigma(0) = 0.11,\ \tau = 9.78]$ for the lower photon energies. The Drude fit is good for photon energies below 1 eV. From this information we may deduce that for low photon energies the conductivity arises due to intra-band transition between the $s-p$ states, which are free electron like and lead to a Drude type behaviour. Above 1 eV there is a onset of inter-band transition between the d and the conduction states and this leads to a sharp increase of optical conductivity and structure reflecting the structures in the d-like states. The inter-band contribution to the imaginary part of the dielectric function $\epsilon_2(\omega)$ may be obtained from the optical conductivity data, by subtracting away the Drude contribution and dividing the result by ω :

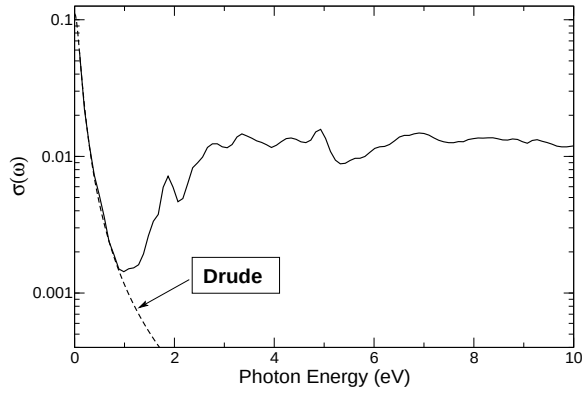


FIG. 3: Averaged optical conductivity showing a Drude fit at low photon energies.

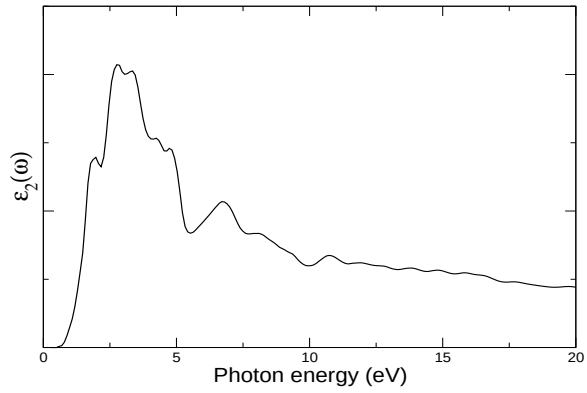


FIG. 4: Inter-band contribution to the imaginary part of the dielectric function for CuAu (50-50) alloy.

$\epsilon_2(\omega) = (\sigma(\omega) - \sigma^D(\omega))/\omega$. Below the onset of the inter-band transitions, this quantity vanishes. It then reaches a maximum at around 3 eV before decreasing. We have experimental data on AgAu (50-50)[6], whose density of states closely resembles CuAu. The experimental data are in good qualitative agreement with Fig. 4. The general shape with a shoulder around 1eV, a maximum and around 3 eV is clearly reproduced.

Figure 5 shows the joint density of states and the averaged correlation function for the NiPt (50-50) alloy. The energy-frequency dependence of the effective transition rate is considerable more pronounced than for CuAu. Disorder correction to the current terms and vertex corrections are also more in the low photon energy region. They become negligible for high photon energies.

Figure 6 shows the density of states and the averaged optical conductivity for NiPt. Although the density of states for NiPt qualitatively resembles that for CuAu, unlike the latter, the Fermi level sits right atop the high peak due to the *d*-like states. The inter-band transitions between the *d*-states and the conduction band is expected to start for very small photon energies, with a Drude contribution confined to a very narrow energy range near zero. The optical conductivity falls sharply in a very

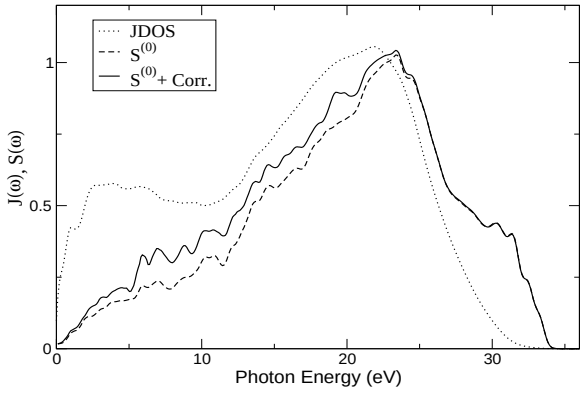


FIG. 5: The configuration averaged joint density of states and correlation function for NiPt (50-50) alloy shown as a function of photon energy.

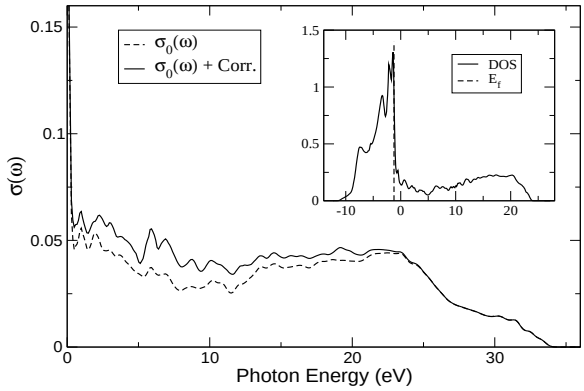


FIG. 6: Averaged optical conductivity and the density of states for NiPt (50-50) alloy.

narrow energy range and recovers almost immediately. This is expected from the density of states picture. Since the Drude fit is in a very narrow range indeed we do not show it explicitly in the figure.

In Fig. 7 we show the inter-band contribution to imagi-

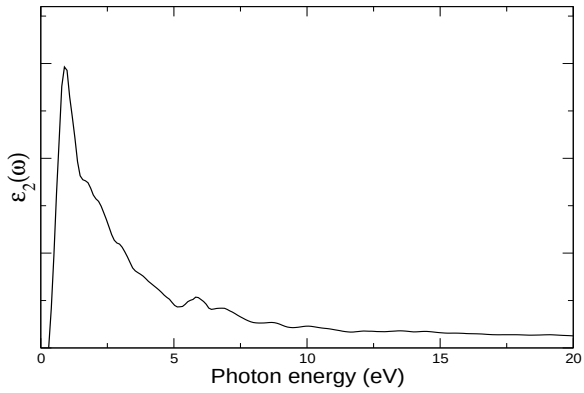


FIG. 7: Inter-band contribution to the imaginary part of the dielectric function for NiPt (50-50) alloy.

nary part of the dielectric function for NiPt (50-50) alloy. The inter-band contribution begins at a very low photon-energy as expected and attains a maximum around 1 eV. This is in contrast to the behaviour of CuAu, where Drude behaviour persists over a longer energy interval. We were unable to locate experimental data for this alloy system for comparison.

III. CONCLUSION

The frequency dependent transport quantities of two disordered metallic alloys have been investigated applying a TB-LMTO-ASR based first principle theory[10]. We have found that the energy-frequency dependence to the effective transition rate is more pronounced for NiPt than that of CuAu. Same tendency was observed in disordered correction to the current terms and vertex corrections in the low photon energy region. We have also found that the conductivity occurs because of both intra-band and inter-band transitions. So the imaginary part of the dielectric function calculated from the conductivity splits into intra and inter-band contributions. For CuAu the intra-band transition takes place up to $\simeq$ 1 eV photon energy and in this region the conductivity curve follows Drude law of free electron model. For NiPt alloy the Drude behaviour is confined to a very narrow energy range, as the Fermi energy straddles the *d*-like peak in density of states. We have compared our results with available theoretical and experimental results and achieved a very impressive agreement with them.

* kamal@bose.res.in
† abhijit@bose.res.in

[1] T. Saha, I. Dasgupta and A. Mookerjee, J. Phys.: Condens. Matter **8** 1979 (1996).
[2] B. Velický, Phys. Rev. **184** 614 (1963).
[3] W. H. Butler, Phys. Rev. B **31** 3260 (1985).
[4] J. Banhart, Phys. Rev. Lett. **82** 2139 (1999).
[5] J. Rivory, Phys. Rev. B **15** 3119 (1977).
[6] P. O. Nielsson, Phys. Kondens. Matter **11** 1 (1970).
[7] J. Y. Rhee, Y. V. Kudryavtsev, K. W. Kim and Y. P. Lee, J. Appl. Phys. **87** 5887 (2000).
[8] L. Uba, S. Uba, V. N. Antonov, A. N. Yaresko and R. Gontarz, Phys. Rev. B **64** 125105 (2001).
[9] J. Y. Rhee, Y. V. Kudryavtsev and Y. P. Lee, Phys. Rev. B **68** 045104 (2003).
[10] K. K. Saha and A. Mookerjee, Phys. Rev. B **70** (2004) (in press) or, cond-mat/0403456.
[11] O. K. Andersen, Phys. Rev. B **12** 3060 (1975).
[12] O. Jepsen and O. K. Andersen, Solid St. Commun. **9** 1763 (1971).
[13] A. Mookerjee, *J. Phys. C: Solid State Phys.* **6** 1340 (1973).
[14] S. Ghosh, N. Das and A. Mookerjee, Int. J. Mod. Phys. B **21**, 723 (1999).